Fluid-Mineral Interactions: A Tribute to H. P. Eugster
© The Geochemical Society, Special Publication No. 2, 1990
Editors: R. J. Spencer and I-Ming Chou

Cassiterite solubility and tin speciation in supercritical chloride solutions

GLENN A. WILSON* and HANS P. EUGSTER†
Department of Earth and Planetary Sciences, The Johns Hopkins University, Baltimore, Maryland 21218, U.S.A.

Abstract—In order to model the evolution of hydrothermal cassiterite deposits, a quantitative understanding of the chemistry of cassiterite-fluid reactions under supercritical conditions is needed. To obtain this information, the solubility of cassiterite in HCl solutions was measured in closed-system experiments from 400 to 700°C, 1.5 kb, with the oxygen fugacity controlled by nickel-nickel oxide (NNO) and hematite-magnetite (HM). From the measured total chloride and tin concentrations, and the conditions of electrical neutrality at P and T, a set of equations was established for each run. By solving the equations simultaneously and finding the best-fit solution for all runs at the same set of P and T conditions, data were obtained on the identity of the dominant aqueous tin-chloride species and the equilibrium constants for the cassiterite dissolution reaction,

$$SnO_2 + XH^+ + nCl^- \rightleftarrows SnCl_n^{X-n} + \frac{X}{2} H_2O + \frac{4 - X}{4} O_2,$$

where X is the oxidation state of aqueous tin and n is the ligation number of the tin-chloride species.

With the f_{O_2} of NNO at 400 to 600°C, it was found that $SnCl^+$ and $SnCl_2^0$ are dominant in solution, and at 700°C only $SnCl_2^0$ was detected. With the f_{O_2} of HM at 500 and 600°C, $SnCl_3^+$ was found to be dominant. The equilibrium constants for the cassiterite dissolution reaction are given by

$$\log K = -3.217 + \frac{2.640 \times 10^4}{T} - \frac{2.143 \times 10^7}{T^2},$$

for X = 2 and n = 1 (T in Kelvin);

$$\log K = 70.080 - \frac{8.246 \times 10^4}{T} + \frac{1.891 \times 10^7}{T^2},$$

for X = 2 and n = 2; and

$$\log K = 59.064 - \frac{3.511 \times 10^4}{T},$$

for X = 4 and n = 3.

The bivalent species dominate under natural ore-forming conditions. The solubility of cassiterite is a strong function of temperature, f_{O_2}, and pH. In order to obtain significant concentrations of tin in solution it is necessary to have temperatures above about 400°C, f_{O_2}'s at or below those defined by NNO, and pH's at or below those defined by the K-feldspar + muscovite + quartz assemblage. Appropriate changes in any of these conditions can cause cassiterite precipitation. The experimental results are in general agreement with studies of natural systems where the high temperature, low pH, and low f_{O_2} environment is indicated by phase relations and fluid inclusion data.

INTRODUCTION

CASSITERITE, SnO_2, is the principle ore mineral of tin, and its primary deposits are usually found to be associated with granitic intrusions. The ore may be found within altered portions of the granite, the so-called greisens, or in hydrothermal veins within the granite or the country rock. Some of the best-known deposits are those of Cornwall (southeast England), Erzgebirge (Czechoslovakia), the Iberian Peninsula, Bolivia, Malaysia, Korea, and southeast China. The extensive literature on tin deposits is summarized in books by TAYLOR (1979), ISHIHARA and TAKENOUCHI (1980), EVANS (1982), HALLS (1985), and KWAK (1987). Many individual deposits have been studied in detail with contributions by KELLY and TURNEAURE (1970, Bolivia), BAUMANN *et al.* (1974, Czechoslovakia), SILLITOE *et al.* (1975, Bolivia), KELLY and RYE (1979, Portugal), COLLINS (1981, Tasmania), PATTERSON *et al.* (1981, Tasmania), ZHANG and LI (1981, China), JACKSON *et al.* (1982, England), CLARK *et al.* (1983, Peru), EADINGTON (1983, Australia), BRAY and SPOONER (1983, England), KWAK (1983, Tasmania), VON GRUENEWALDT and STRYDOM (1985, S. Africa), JACKSON and HELGE-

* Present address: Shell Development Company, Bellaire Research Center, P.O. Box 481, Houston, Texas 77001.
† Deceased.

SON (1985b, Malaysia), PETERSON (1986, Canada), PUCHNER (1986, Alaska), SUN and EADINGTON (1987, Australia), and many others. Although an extensive set of data is available now on mineral associations, fluid inclusions, and stable isotopes, little is known with respect to the hydrothermal transport of tin and the factors which initiate and sustain the precipitation of cassiterite and the associated sulfides. This information, which is a crucial ingredient of any genetic model, may be obtained from solubility measurements carried out under carefully controlled conditions. We report here the results of such experiments between 400°C and 700°C at 1.5 kb pressure in the presence of chloride-bearing fluids.

Previous cassiterite solubility determinations at temperatures up to 400°C were carried out in solutions of sodium hydroxide (KLINTSOVA and BARSUKOV, 1973), silicic chloride (NEKRASOV and LADZE, 1973), acidic and alkaline fluoride (KLINTSOVA *et al.*, 1975), and chloride and nitrate (DADZE *et al.*, 1982). Unfortunately, oxygen fugacity was not controlled in these studies, and hence the nature of the tin solutes cannot be established. KOVALENKO *et al.* (1986) measured cassiterite solubility in HCl solutions at 500°C, 1.0 kb with the NNO oxygen fugacity buffer. They interpreted their results in terms of the species, $SnCl_2^0$, for solutions of 0.01–0.50 m HCl. Recently, PABALAN (1986) has measured cassiterite solubility in subcritical solutions.

Cassiterite solubility has been predicted from theoretical considerations. PATTERSON *et al.* (1981) concluded that $SnCl_3^-$ is the most abundant species between 30 and 350°C with minor amounts of $SnCl^+$ and $SnCl_2^0$. EADINGTON (1982) suggested that between 250 and 400°C under acid conditions $SnCl_2^0$ and SnF^+ are dominant, whereas hydroxide species dominate under basic conditions. JACKSON and HELGESON (1985a) found that between 250 and 350°C under slightly acid to alkaline conditions hydroxide complexes of tin predominate, whereas under very acid conditions, $SnCl_2^0$ and $SnCl_3^-$ are abundant. Obviously, these predictions must be checked by direct experiment before they can be used with any degree of confidence.

EXPERIMENTAL PROCEDURES AND RESULTS

General procedures used in solubility and speciation studies have been discussed by WILSON (1986), WILSON and EUGSTER (1984), and EUGSTER *et al.* (1987). To permit speciation calculations, the total metal concentration must be measured as a function of free ligand concentration at pressure and temperature. Multiple regression analysis is used to account for the metal concentration in terms of several metal-ligand species. Alternatively, if only one species is present, a graphical analysis suffices. In order to define solubility with respect to several species, the free ligand concentration must be varied as widely as possible between measurements. Applications of these procedures in room temperature to subcritical hydrothermal solutions have been discussed by ROSSOTTI and ROSSOTTI (1961), JOHANSSON (1970), SEWARD (1973, 1976), CRERAR *et al.* (1978), HARTLEY *et al.* (1980), WOOD and CRERAR (1985), and others.

Experiments carried out under supercritical conditions require special care. Small-volume, sealed noble metal capsules are used, providing usually no more than 80 μl solution. The control of the chemical conditions, such as *p*H, is difficult, and *in situ* conditions cannot be monitored directly. The only measurements that can be made are those done after the system is quenched to room temperature. The *in situ* conditions must then be back-calculated from those measurements. In addition to pressure and temperature, the oxygen fugacity, f_{O_2}, must be controlled, using the appropriate oxygen buffer assemblage. This is particularly important for multivalent metals. In order to minimize back reactions during quench, rapid-quench techniques are used (EUGSTER *et al.*, 1987).

Chloride solutions were chosen for the present study due to their known dominance in ore-forming environments (HAAPALA and KINNUNEN, 1982; COLLINS, 1981; and many others). To keep the solution composition as simple as possible, the experiments were performed in HCl solutions. From these experiments, the dominant tin-chloride speciation and the equilibrium constants for the cassiterite dissolution reactions can be determined. Since tin exists in either the bivalent or quadruvalent state, the reactions that govern the solubility of cassiterite in HCl solutions are

$$SnO_2 + 2H^+ + nCl^- \rightleftarrows SnCl_n^{2-n} + H_2O + \tfrac{1}{2}O_2 \qquad (1,n)$$

and

$$SnO_2 + 4H^+ + nCl^- \rightleftarrows SnCl_n^{4-n} + 2H_2O, \qquad (2,n)$$

where n is the ligand number of an individual mononuclear tin-chloride species and is a small integer. For different ligand concentrations, different species (hence, different values of n) can exist. Also, since there are likely to be more than one species in solution at a given set of conditions, a number

of reactions of this form will represent the system. The equilibrium constants for these reactions are expressed as

$$K_{1,n} = \frac{(SnCl_n^{2-n}) f_{O_2}^{1/2}}{(H^+)^2 (Cl^-)^n} \qquad (3,n)$$

and

$$K_{2,n} = \frac{(SnCl_n^{4-n})}{(H^+)^4 (Cl^-)^n}, \qquad (4,n)$$

where brackets indicate molality at pressure and temperature, and H_2O and SnO_2 are in their standard states of pure liquid and solid, respectively, at P and T. Activity coefficients for the aqueous species are assumed to be unity, which implies a standard state of unit activity at 1 molal concentration of the species in a solution of ionic strength equal to that of the experiments. For this reason, application of the results should be limited to solutions which have total chloride concentrations in the range represented by the experiments. The goal of the experiments described here was to determine the values of n for the most dominant tin-chloride species and the values of the corresponding equilibrium constants, $K_{1,n}$ and $K_{2,n}$.

The experimental setup, shown in Fig. 1, consists of 45 mg reagent grade SnO_2 with 60–80 μl HCl solution, between 0.18 and 3.3 molal, in a sealed gold metal tube (4.0 mm I.D., 4.2 mm O.D, 25 mm long). The oxygen buffer, either hematite-magnetite (HM) or nickel-nickel oxide (NNO), is contained within an inner, sealed platinum metal tube (2.8 mm I.D., 3.0 mm O.D., 15 mm long) together with 25 μl distilled water. This variation of the standard double-tube arrangement (see EUGSTER and WONES, 1962) provides a larger solution volume for analysis and a quicker extraction. Each run was held at temperature and 1.5 kb pressure for between 14 and 90 days in a 30 cm long cold-seal pressure vessel with a 30 cm long rapid-quench extension (see EUGSTER *et al.*, 1987). To effect reversals, run temperature was approached from below in some runs, and from above in the others. For approach from above, the runs were first held at 100°C higher than the final run temperature for 1 day before being brought down to the run temperature.

After a run was quenched, the capsule was cleaned, weighed, and centrifuged at 14,000 G for 40 seconds. It was placed in a glovebox purged with water-saturated argon to prevent oxidation and evaporation. The fluid was extracted and collected on a teflon watchglass. Aliquots of 10 or 20 μl were diluted in volumetric flasks to 5 or 10 ml with 1.2 N HCl for the Sn analysis, and with 10 to 50 ml distilled water for the chloride analysis. The remaining fluid was used to measure pH with a combination microelectrode while still in the glovebox. Chloride concentrations were measured with a Buchler chloridometer and tin with an AA spectrophotometer and graphite furnace. Excellent precision was achieved in the tin analysis by using a stabilized temperature platform, adding 500 ppm $NiNO_3$ to the solution, and adding 10% H_2 to the purge gas (SLAVIN *et al.*, 1981; RAYSON and HOLCOMBE, 1982). The estimated uncertainty in the tin and chloride determinations is estimated to be ±5% based on the number of dilutions and the precision of the measurements. A check on gold concentrations revealed no detectable gold in solution. Results of the successful experiments are listed in Table 1.

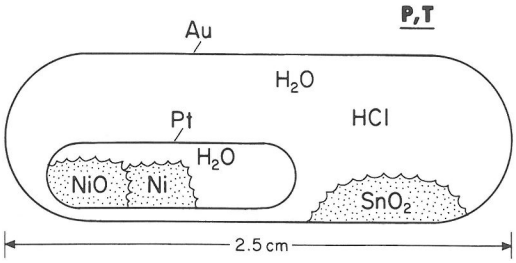

FIG. 1. Schematic diagram of the experimental setup for cassiterite solubility experiments.

INTERPRETATION OF DATA: REGRESSION PROCEDURES

From the measurements of total chloride, total tin, and pH at 25°C, the oxidation state of aqueous tin can be calculated. In these acid solutions, the contribution of OH^- can be neglected, thus, the room-temperature charge balance equation becomes

$$X Sn_{total} + (10)^{-pH_Q} = Cl_{total}, \qquad (5)$$

where X is the oxidation state of aqueous tin, Sn_{total} and Cl_{total} are the tin and chloride concentrations measured after quench, and pH_Q is the pH of the quenched solution. The largest uncertainty in calculating X from Equation (5) arises from the pH measurement (see Table 1), because of the extremely small fluid volume and possible poisoning of the microelectrode by tin ions. Nevertheless, the average value of X at all temperatures is 2.18 ± 0.24 for runs buffered by NNO, and 3.63 ± 0.77 for runs buffered by HM. Due to the uncertainty associated

with this determination, and the lack of a clear relationship between the calculated values of X and Cl_{total}, we assume that only one oxidation state of aqueous tin is present in significant quantities. Note that a mixture of oxidation states is impossible in *both* the HM and NNO runs due to the many orders of magnitude difference in f_{O_2} between these two buffers. Thus, it appears that aqueous tin is bivalent and quadruvalent under the conditions of NNO and HM, respectively.

Because of the use of rapid-quench techniques and the extraction of the fluid under an inert atmosphere, we assume that X is also the oxidation state of tin in solution at P and T. Consequently, once X is known, the electrical neutrality equation at P and T can be expressed as

$$(H^+)^{P,T} + \sum_n [X - n](SnCl_n^{X-n})^{P,T} = (Cl^-)^{P,T}, \quad (6)$$

where the summation is over all species, $SnCl_n^{X-n}$, that exist in solution at significant concentrations. The tin and chloride mass balance at P and T are given by

$$Sn_{total} = \sum_n (SnCl_n^{X-n})^{P,T}, \quad (7)$$

and

$$Cl_{total} = (Cl^-)^{P,T} + (HCl^0)^{P,T} + \sum_n n(SnCl_n^{X-n})^{P,T}. \quad (8)$$

In addition, the dissociation of HCl^0 at P and T yields the following expression:

$$K_{HCl} = \frac{(H^+)^{P,T}(Cl^-)^{P,T}}{(HCl^0)^{P,T}}, \quad (9)$$

(assuming unit activity coefficients) where the values for K_{HCl} are from FRANTZ and MARSHALL (1984). Finally, the dissociation reaction for the n^{th} tin chloride species,

$$SnCl_n^{X-n} \rightleftarrows SnCl_{n-1}^{X-n+1} + Cl^-, \quad (10,n)$$

provides the relation,

$$K_{10,n} = \frac{(SnCl_{n-1}^{X-n+1})^{P,T}(Cl^-)^{P,T}}{(SnCl_n^{X-n})^{P,T}}. \quad (11,n)$$

One equation of this form can be written for each two consecutive tin-chloride species that are proposed to exist in solution. In other words, if a total of m consecutive species are proposed, then there will be m − 1 independent equations of the form of Equation (11,n). Together with Equations (6), (7), (8), and (9), there will be a total of m + 3 equations describing the conditions of each individual run.

Table 1. Conditions and analytical results of cassiterite solubility experiments

Run #	Temp (°C)	Buf.	Dur. (days)	App. dir.	Cl_T (m)	Sn_T (m)	pH_Q	X
40	400	NNO	86	↓	0.654	0.210	0.890	2.50
41	400	NNO	95	↑	1.21	0.435	0.655	2.27
44	400	NNO	86	↓	2.03	0.815	0.658	2.22
45	400	NNO	36	↑	0.642	0.211	0.830	2.34
46	400	NNO	36	↑	2.08	0.793	0.374	2.09
47	400	NNO	35	↑	0.286	0.0790	1.028	2.43
48	400	NNO	30	↓	0.291	0.0910	1.083	2.29
23	500	NNO	41	↑	1.956	0.771	0.503	2.13
24	500	NNO	35	↓	1.854	0.773	0.548	2.03
25	500	NNO	21	↑	0.191	0.0710	1.440	2.18
28	500	NNO	18	↓	0.610	0.222	1.261	2.50
29	500	NNO	22	↑	1.14	0.461	0.875	2.18
49	500	NNO	32	↑	0.696	0.257	0.938	2.26
50	500	NNO	27	↓	1.19	0.511	0.804	2.02
51	500	NNO	27	↓	0.200	0.0794	1.384	2.00
62	500	NNO	19	↑	4.82	2.01	≤0	≤1.9
76	500	NNO	54	↑	3.23	1.27	0.250	2.10
77	500	NNO	44	↓	3.13	1.33	0.245	1.93
70	500	NNO	33	↑	0.305	0.0586	0.872	2.92
72	500	NNO	33	↑	1.25	0.318	0.354	2.54
73	500	NNO	22	↓	1.21	0.329	0.360	2.35
74	600	NNO	33	↑	4.45	1.84	0.160	2.04
75	600	NNO	23	↓	4.36	1.75	N.D.	—
84	600	NNO	43	↑	0.302	0.599	0.793	2.36
85	600	NNO	34	↓	1.11	0.303	0.258	1.83
100	600	NNO	15	↓	0.614	0.141	0.531	2.27
101	600	NNO	15	↓	2.49	0.800	0.092	2.10
90	700	NNO	9	↑	1.21	0.261	0.242	2.44
91	700	NNO	9	↑	4.45	1.49	≤0	≤2.3
53	500	HM	29	↑	1.15	0.225	0.372	3.21
64	500	HM	36	↑	0.174	0.0195	1.021	4.05
66	500	HM	36	↑	0.794	0.142	0.398	2.78
67	500	HM	30	↓	1.02	0.172	N.D.	—
69	500	HM	30	↓	3.01	0.652	N.D.	—
82	600	HM	43	↑	2.39	0.320	≤0	≤4.3
86	600	HM	10	↑	0.300	0.0107	N.D.	—
87	600	HM	10	↑	1.20	0.120	0.180	4.48
88	600	HM	10	↑	4.64	0.682	≤0	≤5.3

Oxygen buffer (Buf.): NNO = nickel-nickel oxide; HM = hematite-magnetite. Dur. = number of days at temperature. App. dir. = direction of approach in temperature. Sn_T and Cl_T are the total measured concentrations of tin and chloride. pH_Q is the pH measured after quench. N.D. = not determined. ≤0 = off scale at zero pH. X is the valence of aqueous tin from Equation (5).

In this set of equations, however, there are 2m + 2 unknowns for each run: $(Cl^-)^{P,T}$, $(H^+)^{P,T}$, $(HCl^0)^{P,T}$, $(SnCl_{n_1}^{X-n_1})^{P,T}$, . . . , $(SnCl_{n_m}^{X-n_m})^{P,T}$, and K_{10,n_1+1}, . . . , K_{10,n_m}. A set of runs at the same pressure and temperature must then be considered as a whole, and the equations solved by nonlinear least squares regression. Since the unknown K_{10}'s are constant for a set of runs at a given P and T, the regression is expressed by m − 1 equations of the form

$$\frac{d\sigma^2}{d(\log K_{10,n})} = 0 \quad (12)$$

which expresses the condition of least squares best fit (BEVINGTON, 1969; DRAPER and SMITH, 1981). Using the case where X = 2 as an example, the standard deviation, σ, is defined by

$$\sigma^2 = \frac{1}{R}\sum_{i=1}^{R}[\log K^i_{1,n} - \log \bar{K}_{1,n}]^2, \quad (13)$$

where $K^i_{1,n}$ is the value of the equilibrium constant for Reaction (1) as determined by run i, $\bar{K}_{1,n}$ is the mean value for all runs at the same pressure and temperature, and R is the total number of runs under that set of conditions. The standard deviation is the same if it is defined in terms of log $K_{1,n}$ (as in Equation 13), log $K_{1,n-1}$ or log Sn_{total}. Thus, the standard deviation is independent of m and can be compared between trials of the calculation where different species, and different numbers of species, are considered. With equations of the form of (11,n) and (12), and Equations (6), (7), (8), and (9), there are 2m + 2 equations, and the system is fully defined.

This regression analysis can be expressed as

$$\log K^i_{1,n} = f(K_{10,n}, Sn^i_{total}, Cl^i_{total}), \quad (14)$$

with log $K_{1,n}$ (or log $K_{2,n}$ if X = 4) as the response variable, $K_{10,n}$ as the regression parameter, and Sn^i_{total} and Cl^i_{total} as the predictor variables from each individual run i. The function, f, represents the combination of Equations (3 or 4), (6), (7), (8), (9), and (11,n), but due to the nature of this set of equations, it cannot be expressed explicitly as a simple regression equation. The analysis can be performed, however, by repeatedly solving the equations (function f) for different values of $K_{10,n}$ until a minimum is found in σ. The solution where σ is at a minimum will yield the best-fit values for the unknowns.

INTERPRETATION OF DATA: INITIAL SPECIES SELECTION

In order to minimize computational difficulty and to avoid over-fitting the data, it is helpful to initially identify the most important species in this system under the temperature and pressure conditions of interest. To do this, Equations (6) through (12) are simplified by assuming that only a single species is present (i.e., m = 1) in a set of runs. The equations are solved for the set of runs considering each possible species, one at a time, and the fits of the results are compared.

With only one species, Reaction (10) is undefined as are Equations (11,n) and (12). Equations (6), (7), (8), and (9) define the system completely for the unknowns $(H^+)^{P,T}$, $(Cl^-)^{P,T}$, $(HCl^0)^{P,T}$, and the concentration of the single tin-chloride species, $(SnCl_n^{X-n})^{P,T}$. The best value of n is found by minimizing the standard deviation as a function of the species chosen, or n. This will be illustrated graphically here. Equations (3) and (4) can be rearranged to the following form:

$$\log\left[\frac{(SnCl_n^{2-n})f_{O_2}^{1/2}}{(H^+)^2}\right] = n\log(Cl^-) + \log K_{1,n}, \quad (15)$$

and

$$\log\left[\frac{(SnCl_n^{4-n})}{(H^+)^4}\right] = n\log(Cl^-) + \log K_{2,n}, \quad (16)$$

where all terms are at P and T. Equations (15) and (16) describe straight lines of slope n. Figure 2 shows the run data for 400°C, buffered by NNO (where X = 2) where Equations (6) through (9) are solved assuming the presence of Sn^{2+} (a), $SnCl^+$ (b), and $SnCl_2^0$ (c). A line of slope n is positioned by using log $\bar{K}_{1,n}$ as the y-intercept. Figure 2(a) shows that the data do not fit the model of Sn^{2+} (n = 0) as the dominant tin-chloride species. In Fig. 2(b), the trend of the points is slighly steeper than the reference line, and in Fig. 2(c), it is slightly shallower. Thus, the mean value of n is between 1 and 2 and it is concluded that significant amounts of $SnCl^+$ and $SnCl_2^0$ are present in solution at 400°C. This is also indicated by the standard deviations which are approximately equal for n = 1 and n = 2, and lower than for n = 0.

The same conclusions can be drawn for the data at 500°C, NNO (Fig. 3) and 600°C, NNO (Fig. 4), although the standard deviations show a slight preference for n = 1 at 500°C and n = 2 at 600°C. Thus, a final model must include both $SnCl^+$ and $SnCl_2^0$ at these temperatures as well. At 700°C, NNO (Fig. 5), the only reasonable fit of the two data points is for n = 2. The ratio of Cl_{total} to Sn_{total} for most of these runs does not permit n = 3.

Under the conditions of HM (where X = 4) at 500 and 600°C, Figs. 6 and 7 indicate that $SnCl_3^+$ is dominant.

INTERPRETATION OF DATA: FINAL SPECIATION CALCULATIONS

Knowing that $SnCl^+$ and $SnCl_2^0$ are the species of interest at 400 to 700°C and NNO, both can be considered simultaneously. The results will yield $K_{1,1}$ for the reaction

$$SnO_2 + 2H^+ + Cl^- \rightleftarrows SnCl^+ + H_2O + \tfrac{1}{2}O_2 \quad (1,1)$$

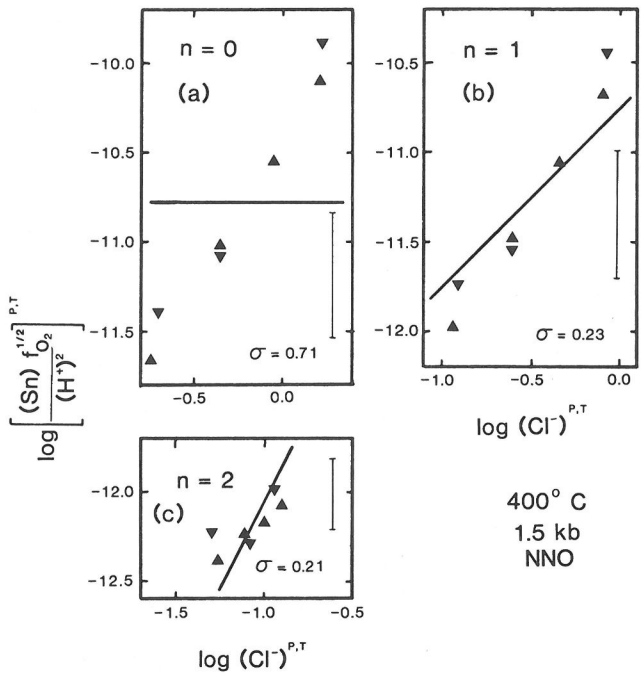

FIG. 2. Experimental cassiterite solubility results at 400°C, 1.5 kb, and NNO (oxidation state of tin is 2). Results for each run are calculated by Equations (6), (7), (8), and (9) and are plotted according to Equation (15). Only one tin-chloride species is considered to be present: Sn^{2+} (n = 0) in (a); $SnCl^+$ (n = 1) in (b); and $SnCl_2^0$ (n = 2) in (c). The total concentration of tin is represented by (Sn). The slope of the line in each diagram conforms to the chosen value of n. Triangles point in the direction of approach to equilibrium (from higher or lower temperature). The standard deviation, σ, is defined by Equation (13). The average estimated experimental error bar is shown on the right-hand side of each diagram and is based on the estimated 5% uncertainty in the tin and chloride measurements (the error in the horizontal direction is smaller than the size of the symbols).

and $K_{1,2}$ for the reaction

$$SnO_2 + 2H^+ + 2Cl^- \rightleftarrows SnCl_2^0 + H_2O + \tfrac{1}{2}O_2. \qquad (1,2)$$

Equations (6), (7), (8), and (9) are written with $SnCl^+$ and $SnCl_2^0$ as the aqueous tin species and Equation (11,n) takes the form of

$$K_{10,2} = \frac{(SnCl^+)^{P,T}(Cl^-)^{P,T}}{(SnCl_2^0)^{P,T}}. \qquad (11,2)$$

Combined, these 5 equations can be solved for the unknowns of an individual run at P and T, $(SnCl^+)^{P,T}$, $(SnCl_2^0)^{P,T}$, $(H^+)^{P,T}$, $(Cl^-)^{P,T}$, $(HCl^0)^{P,T}$, provided that a value is assumed for $\log K_{10,2}$.

For a set of runs, the procedure is to assume a value of $\log K_{10,2}$, solve the set of equations for each run, and calculate σ by Equation (13). This is done repeatedly using different values of $\log K_{10,2}$ until a minimum is found in σ, and Equation (12) is satisfied. The minimum indicates the best fit of the data to the two-species model.

The regression analysis is illustrated in Fig. 8 where σ is plotted against different assumed values of $\log K_{10,2}$. At 400, 500, and 600°C, the calculations yield a distinct minimum in σ at $\log K_{10,2} = -0.45$, 0.16, and -1.35, respectively. This confirms that, statistically, the best fit of these experimental data is for a model where a combination of both $SnCl^+$ and $SnCl_2^0$ is present. As the assumed value of $\log K_{10,2}$ is made larger or smaller, σ increases rapidly before finally leveling off at the value obtained when only one species is assumed to be present ($SnCl^+$ or $SnCl_2^0$, respectively). For the 700°C data, σ decreases rapidly as the assumed value of $\log K_{10,2}$ is decreased to about -3.75. At that point, σ nearly reaches its lowest value; approximately that obtained when only $SnCl_2^0$ was assumed to be present. As the assumed value of $\log K_{10,2}$ is made smaller, σ continues to decrease, but only very slightly, while the resulting $\log K_{1,2}$ remains constant. Thus, at 700°C, it can be concluded that $SnCl_2^0$ is dominant in this concentration range and that the maximum amount of $SnCl^+$ compatible with the data is determined by $\log K_{1,1} \leq \log K_{1,2} + (-3.75)$.

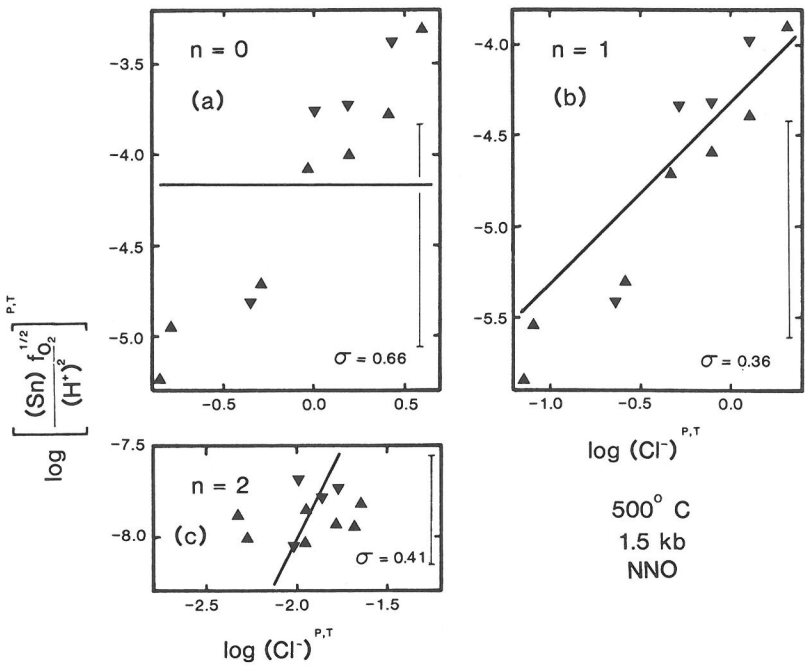

FIG. 3. Experimental cassiterite solubility results at 500°C, 1.5 kb, and NNO (oxidation state of tin is 2). See Fig. 2 caption.

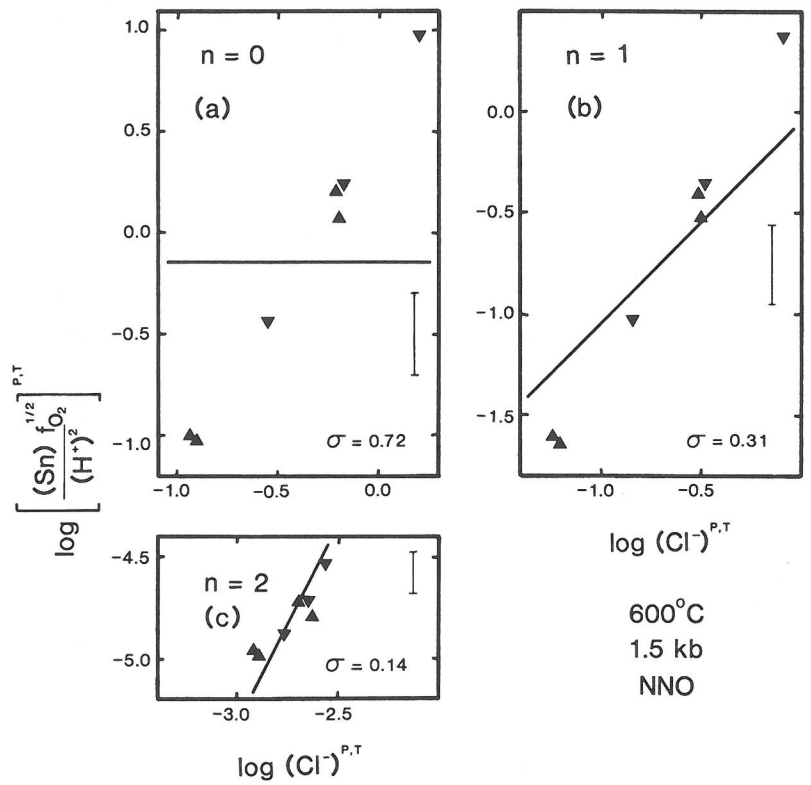

FIG. 4. Experimental cassiterite solubility results at 600°C, 1.5 kb, and NNO (oxidation state of tin is 2). See Fig. 2 caption.

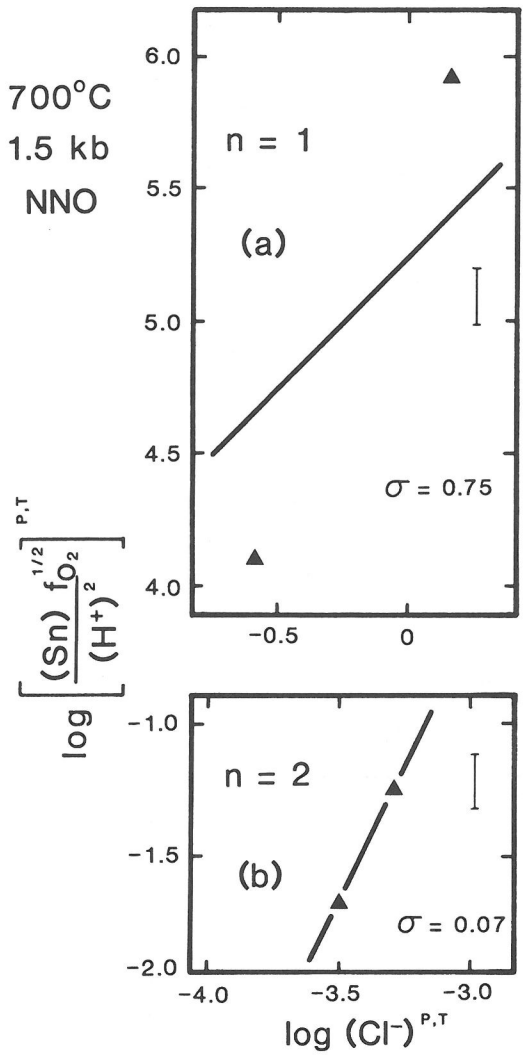

FIG. 5. Experimental cassiterite solubility results at 700°C, 1.5 kb, and NNO (oxidation state of tin is 2). See Fig. 2 caption.

The best-fit results are listed in Table 2. These are illustrated in Fig. 9 for 400°C (a), 500°C (b), 600°C (c), and 700°C (d), at 1.5 kb and NNO. Again, as in Figs. 2 through 7, the solubility diagram as defined by Equation (15) is used where the data points represent the total solubility of cassiterite calculated for each run. The bold curve is the best-fit curve through the points and is determined by both $\log \bar{K}_{1,1}$ and $\log \bar{K}_{1,2}$. It is the sum of the two lighter lines shown for the individual species, $SnCl^+$ and $SnCl_2^0$.

Figure 9(a, b, and d) shows that there is no strong systematic deviation of the points from the mean at 400, 500, and 700°C. This is an indication that no tin-chloride species other than the two considered are present in detectable amounts. At 600°C (Fig. 9c), however, the two points to the far right (open triangles) which lie above the mean suggest that a third species, $SnCl_3^-$, may be present at the highest chloride concentrations. These two runs were not included in the regression analysis. Addition of this third species would probably not significantly change the values obtained for $\log K_{1,1}$ and $\log K_{1,2}$.

The best-fit values of $\log K_{10,2}$ and the mean values determined for $\log K_{1,1}$ and $\log K_{1,2}$ are listed in Table 3. The uncertainties shown are based on the estimated errors in the Cl_{total} and Sn_{total} measurements which are carried through the entire calculation by the standard method of error propagation (REES, 1984; BEVINGTON, 1969).

For the experimental data from runs buffered by HM where X = 4 at 500 and 600°C, the fit to the one-species model ($SnCl_3^+$) is as good as can be expected. No attempt was made to improve the fit by the addition of other species to the calculations. The mean values for $\log K_{2,3}$ as determined in the previous section are also given in Table 3.

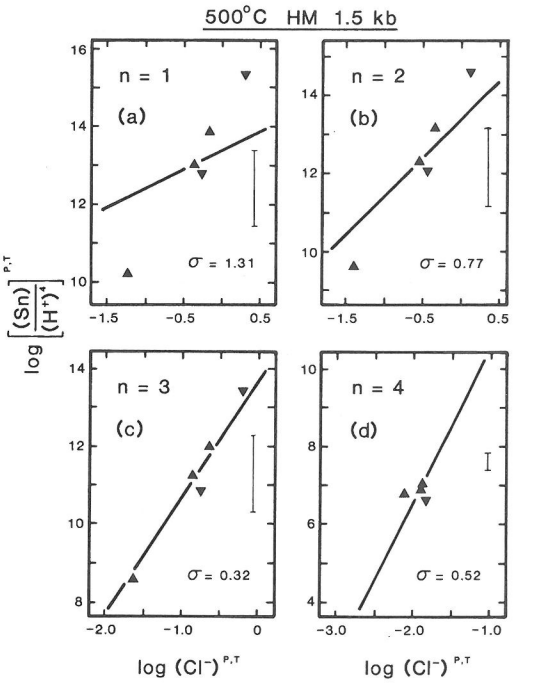

FIG. 6. Experimental cassiterite solubility results at 500°C, 1.5 kb, and HM (oxidation state of tin is 4). See Fig. 2 caption for explanation. One species is considered to be present: $SnCl^{3+}$ (n = 1) in (a); $SnCl_2^{2+}$ (n = 2) in (b); $SnCl_3^+$ (n = 3) in (c); and $SnCl_4^0$ (n = 4) in (d). In one of the runs (#69) no solution could be obtained for n = 4.

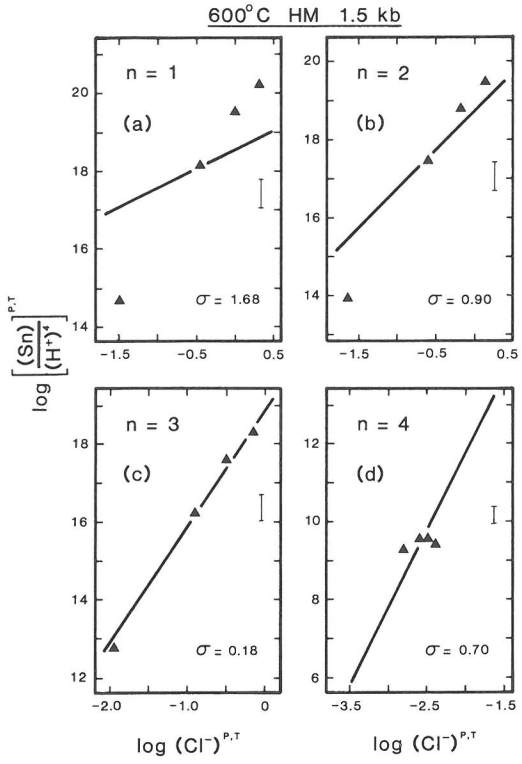

FIG. 7. Experimental cassiterite solubility results at 600°C, 1.5 kb, and HM (oxidation state of tin is 4). See captions for Figs. 2 and 6.

THERMODYNAMIC PARAMETERS

The equilibrium constants determined in this study can be represented as a function of temperature by an equation of the form

$$\log K = a + \frac{b}{T} + \frac{c}{T^2} \qquad (17)$$

where the coefficients a, b, and c are determined by least-squares regression of the data in Table 3 and T is in Kelvin. The coefficients for Reactions 1,1; 1,2; 2,3; and 10,2 are given in Table 4.

In Fig. 10, log K is plotted against $1/T(K)$ for Reactions 1,1; 1,2; and 10,2. The uncertainties in log K are less than or equal to the size of the symbols. The regression curve as defined by Equation (17) is also shown. The non-unique solutions for log $K_{1,1}$ and log $K_{10,2}$ at 700°C are the maximum possible values. These were not used in determining the regression curves but are included in Fig. 10 to show that they are compatible with the extrapolations of the lower temperature data.

For comparison, the data of PATTERSON *et al.* (1981) and JACKSON and HELGESON (1985a) at 350°C and pressure equal to the saturated vapor pressure of water (P_{sat}) are also plotted in Fig. 10. Although the difference in pressure makes this comparison only approximate, there is reasonable agreement in the value for log $K_{10,2}$. Shown also is the value for log $K_{1,2}$ at 500°C, 1.0 kb from KOVALENKO *et al.* (1986) which shows reasonable agreement as well.

The results for log $K_{10,2}$ as a function of temperature can be used to derive information on the thermodynamics of complex dissociation. The slope of the lower curve in Fig. 10 is related to the standard enthalpy of reaction, $\Delta H^0_{10,2}$, by the equation

$$\frac{d \log K_{10,2}}{d(1/T)} = \frac{-\Delta H^0_{10,2}}{(2.303)R}, \qquad (18)$$

where R is the gas constant and T is in Kelvin. The entropy of reaction, $\Delta S^0_{10,2}$, is given by

$$\Delta S^0_{10,2} = \frac{\Delta H^0_{10,2}}{T} + (2.303)R \log K_{10,2}. \qquad (19)$$

The resulting values of $\Delta H^0_{10,2}$ and $\Delta S^0_{10,2}$ are listed in Table 5. It can be seen that $\Delta H^0_{10,2}$ and $\Delta S^0_{10,2}$ are both positive at 400°C and negative at temperatures of 500°C and above. There is a systematic decrease in both $\Delta H^0_{10,2}$ and $\Delta S^0_{10,2}$ with increasing temperature from 400 to 700°C. As discussed by SEWARD (1981), this reflects the changing nature of the solvent, the hydration of the charged species, and the chemical bonding between the metal ion and the ligand. The positive enthalpy at 400°C is indicative of predominantly covalent bonding. The charged species are not strongly solvated under these conditions and relatively little water is involved in the reaction. Thus, a small positive entropy is caused by an increase in the number of particles and an increased vibrational and rotational energy in the system. At 500°C and above, the increasingly negative entropy values are indicative of an increase in the electrostatic (ionic) character of the bonding with temperature. The negative $\Delta S^0_{10,2}$ values indicate that what solvation water *is* involved in the reaction is derived from an increasingly disordered solvent.

GEOLOGIC APPLICATIONS

Data presented here can be used to predict the oxidation state of aqueous tin, the nature of the aqueous tin-chloride complexes in natural environments, the solubility of cassiterite in ore fluids, and mechanisms likely to cause cassiterite precipitation. The physical and chemical conditions existing at the time of cassiterite deposition, such as f_{O_2}, T, pH, and salinity, can be estimated from mineralogical, fluid inclusion, and isotopic studies.

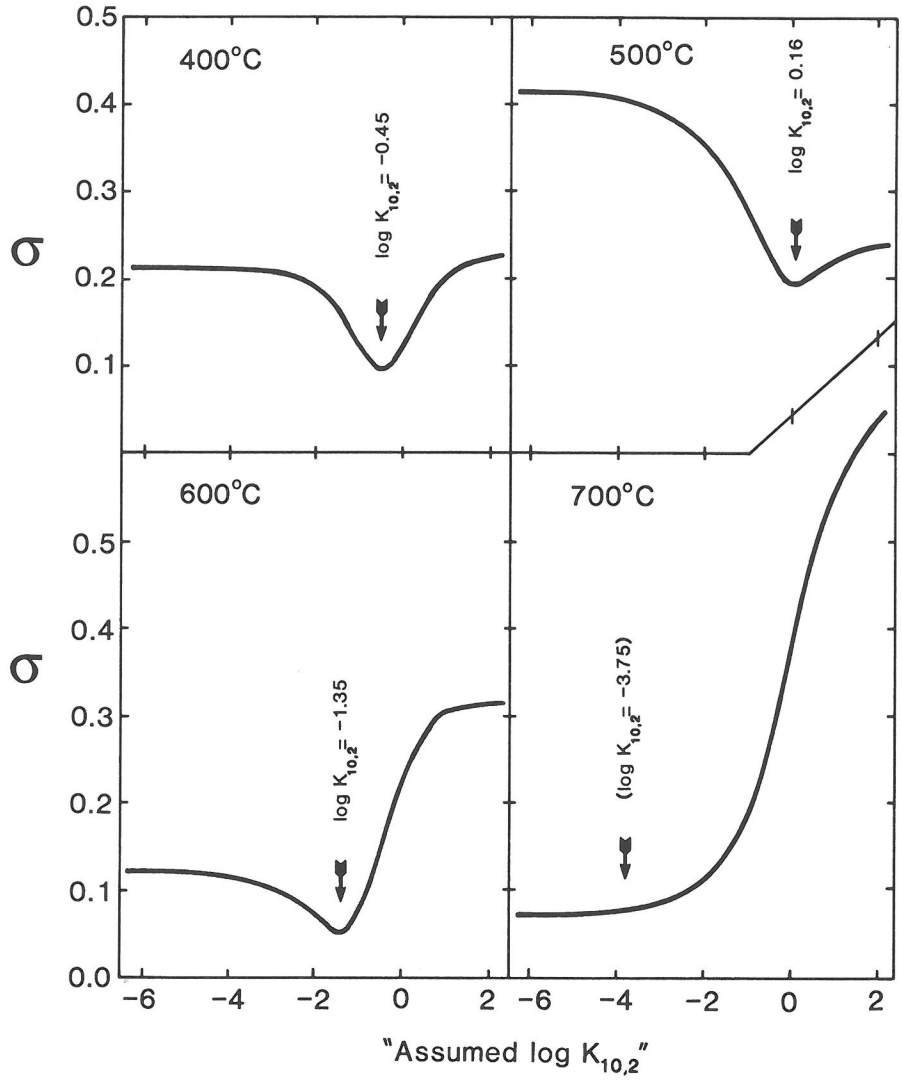

FIG. 8. The standard deviation as defined by Equation (13) plotted against assumed values for log $K_{10,2}$. A minimum in the curve is where Equation (12) is satisfied and indicates the value of log $K_{10,2}$ which best fits the experimental data. No minimum is found at 700°C, but the largest permissible value of log $K_{10,2}$ is indicated (see text).

Acidic conditions are indicated by the common occurrence of acid-alteration assemblages in cassiterite deposits, such as greisenization of granitic host-rock, alteration of feldspars to muscovite, alteration of biotite to muscovite or chloride in schists, and the formation of skarns in carbonate rock. These alterations set an upper limit on the pH of the ore-forming fluids at below neutral near the site of deposition, although the fluids could be more acidic at their source. Individual studies of fluid inclusions and phase relations indicate that mineralizing fluids had pH values in the range of 3.9 to 5.4 at the site of ore deposition (PATTERSON *et al.*, 1981; JACKSON and HELGESON, 1985b).

Oxygen fugacities of the ore-forming fluids at Renison Bell, Tasmania were estimated by PATTERSON *et al.* (1981) using CO_2/CH_4 ratios in fluid inclusions, and at Mt. Lindsay, Tasmania by KWAK (1983) using a rare occurrence of iron-titanium oxides. They found values between those defined by the NNO and QFM buffers. Topaz rhyolites associated with small cassiterite deposits in the western United States have f_{O_2} values approximately equal to those defined by the QFM buffer (CHRISTIANSEN

Table 2. Best-fit results of cassiterite solubility data

Run	log ($SnCl^+$)	log ($SnCl_2^0$)	log (Cl^-)	log (H^+)	log $K^i_{1,1}$	log $K^i_{1,2}$
			400°C, NNO (log f_{O_2} = −27.572)			
40	−0.858	−1.146	−0.738	−1.355	−11.196	−10.746
41	−0.618	−0.713	−0.545	−1.356	−11.147	−10.697
44	−0.424	−0.358	−0.383	−1.429	−10.970	−10.520
45	−0.855	−1.146	−0.741	−1.379	−11.141	−10.691
46	−0.436	−0.370	−0.384	−1.336	−11.165	−10.715
47	−1.210	−1.761	−1.001	−1.418	−11.160	−10.710
48	−1.151	−1.690	−0.989	−1.496	−10.957	−10.507
			500°C, NNO (log f_{O_2} = −22.796)			
23	−0.255	−0.669	−0.254	−3.323	−4.752	−4.912
24	−0.254	−0.667	−0.253	−3.452	−4.494	−4.654
25	−1.169	−2.495	−1.166	−3.346	−4.709	−4.869
28	−0.709	−1.577	−0.708	−3.267	−4.865	−5.025
29	−0.435	−1.030	−0.435	−3.429	−4.540	−4.700
49	−0.652	−1.464	−0.651	−3.283	−4.832	−4.992
50	−0.398	−0.955	−0.397	−3.569	−4.260	−4.420
51	−1.122	−2.403	−1.120	−3.462	−4.476	−4.636
62	0.053	−0.055	0.053	−3.343	−4.711	−4.871
76	−0.090	−0.340	−0.090	−3.265	−4.868	−5.028
77	−0.075	−0.310	−0.075	−3.447	−4.505	−4.665
			600°C, NNO (log f_{O_2} = −19.113)			
70	−1.475	−1.600	−1.475	−4.315	−0.928	0.422
72	−1.005	−0.659	−1.005	−4.270	−1.016	0.334
73	−0.996	−0.642	−0.996	−4.325	−0.906	0.444
84	−1.469	−1.587	−1.468	−4.334	−0.890	0.460
85	−1.017	−0.684	−1.017	−4.346	−0.864	0.486
100	−1.221	−1.092	−1.221	−4.321	−0.915	0.435
101	−0.775	−0.199	−0.775	−4.340	−0.877	0.473
			700°C, NNO (log f_{O_2} = −16.187)			
90	(−2.173)	−0.595	−2.172	−4.825	(1.555)	5.305
91	(−1.791)	0.169	−1.790	−4.878	(1.662)	5.412

Run	log ($SnCl_3^+$)	log (Cl^-)	log (H^+)	log $K^i_{2,3}$
		500°C, HM		
53	−0.648	−0.646	−3.151	13.892
64	−1.710	−1.653	−2.567	13.516
66	−0.848	−0.845	−2.993	13.660
67	−0.764	−0.761	−2.912	13.165
69	−0.186	−0.185	−3.398	13.959
		600°C, HM		
82	−0.495	−0.495	−4.520	19.069
86	−1.971	−1.962	−3.688	18.666
87	−0.921	−0.921	−4.283	18.973
88	−0.166	−0.166	−4.613	18.782

All concentrations are for the species at 1.5 kb and T. Parentheses indicate maximum permitted values at 700°C (see text).

et al., 1986). HAAPALA and KINNUNEN (1982) summarized published data on fluid inclusions in cassiterite from tin deposits around the world. They found that the most common values for homogenization temperatures were in the range of 300 to 400°C, but some were as high as 500°C and a few were as low as 250°C. They point out that when corrected for pressure, the depositional tempera-

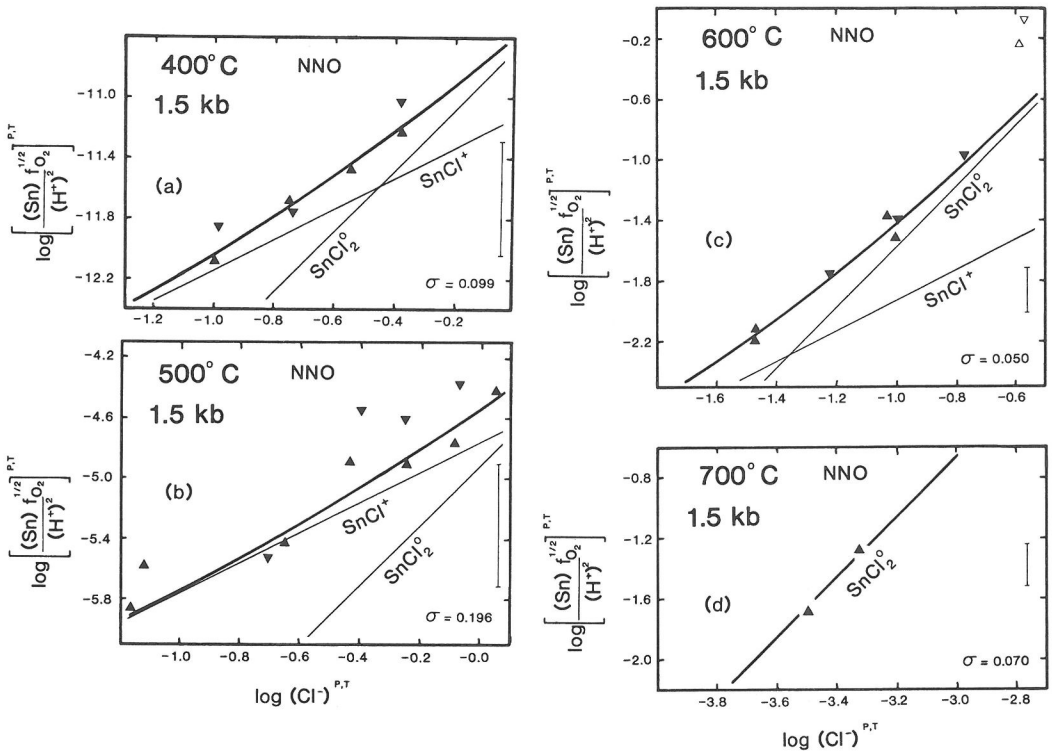

FIG. 9. Experimental cassiterite solubility at 400 (a), 500 (b), 600 (c), and 700°C (d), all at 1.5 kb and NNO (oxidation state of tin is 2). Each point represents the best-fit solution of Equations (6), (7), (8), (9), (11,2), and (12) as discussed in the text and Fig. (8). The standard deviation, σ, is defined by Equation (13). The average estimated error bar is shown on the right-hand side of each diagram and is based on the estimated 5% uncertainty in the tin and chloride measurements (uncertainty in the horizontal direction is smaller than the size of the symbols). See text for explanation of the two runs at 600°C represented by open symbols.

tures could be 100°C or more higher than the homogenization temperatures.

Salinities of ore-forming fluids as determined by fluid inclusion studies of cassiterite deposits are variable, ranging from about 1 m NaCl equivalent to as high as 8 m (HAAPALA and KINNUNEN, 1982; ROEDDER, 1984). Most commonly, however, during the stage of cassiterite formation, salinities were in the range of 1 to 2 m (KELLY and RYE, 1979; COLLINS, 1981; PATTERSON *et al.*, 1981; ZAW and DAW, 1983; JACKSON and HELGESON, 1985b; JACKSON *et al.*, 1982; NORMAN and TRANGCOTCHASAN, 1982). Estimates of fluid pressures range from 100 to 1800 bars (HAAPALA and KINNUNEN, 1982).

Table 3. Best-fit equilibrium constants for Reactions (1,1), (1,2), (10,2), and (2,3)

T (°C)	400	500	600	700
$\log K_{1,1}$	−11.14	−4.76	−0.93	(1.58)
	±0.15	±0.21	±0.06	(±0.09)
$\log K_{1,2}$	−10.69	−4.92	0.42	5.33
	±0.16	±0.22	±0.07	±0.10
$\log K_{10,2}$	−0.45	0.16	−1.35	(−3.75)
$\log K_{2,3}$	—	13.64	18.87	—
		±0.25	±0.16	

To obtain the relationship between stannous and stannic chloride complexes in hydrothermal fluids, Reactions (1,1) and (1,2) can be combined with Reaction (2,3) to yield the following:

$$SnCl^+ + 2Cl^- + 2H^+ + \tfrac{1}{2}O_2 \rightleftarrows SnCl_3^+ + H_2O \quad (20)$$

and

$$SnCl_2^0 + Cl^- + 2H^+ + \tfrac{1}{2}O_2 \rightleftarrows SnCl_3^+ + H_2O. \quad (21)$$

The equilibrium constants for these reactions can be obtained by combining the data listed in Table 4:

Table 4. Coefficients for Equation (17) for Reactions (1,1), (1,2), (10,2), and (2,3)

Reaction	a	b	c
(1,1)	−3.217	2.640×10^4	-2.143×10^7
(1,2)	70.080	-8.246×10^4	1.891×10^7
(10,2)	−70.812	1.054×10^5	-3.904×10^7
(2,3)	59.064	-3.511×10^4	—

$$\log K_{20} = 62.28 - \frac{6.15 \times 10^4}{T} + \frac{2.14 \times 10^7}{T^2} \quad (22)$$

and

$$\log K_{21} = -11.02 + \frac{4.74 \times 10^4}{T} - \frac{1.89 \times 10^7}{T^2} . \quad (23)$$

Equations (22) and (23) are only valid at 500 and 600°C because Reaction (2,3) was only determined at these temperatures. The relation between stannous and stannic chloride species depends on chloride ion concentration, pH, and f_{O_2}. To evaluate the relative importance of these two oxidation states of aqueous tin in natural fluids, Equations (22) and (23) were used to plot the boundary between stannous chloride dominance and stannic chloride dominance. This is shown in Fig. 11 as a function of f_{O_2} and T for a 2 m Cl_{total} fluid in equilibrium with the assemblage K-feldspar + muscovite + quartz. This assemblage is commonly associated with cassiterite deposits, and at a given KCl concentration, it fixes the pH of the fluid. For reference, the oxygen buffer curves for HM and QFM are also shown. The boundary between stannous and stannic dominance lies well above the region of f_{O_2} typical of cassiterite-bearing fossil hydrothermal systems. Thus, only the stannous species are expected to be found in such systems. This conclusion holds even if the pH is as much as 1.5 units lower. The species $SnCl^+$ and $SnCl_2^0$ then, are the tin-chloride species of importance under most natural hydrothermal conditions.

The total solubility of cassiterite as a function of temperature is plotted in Fig. 12 at the oxygen buffers QFM, NNO, HM. Again, it was assumed that a fluid of 2 m Cl_{total} is in equilibrium with the acid buffer assemblage K-feldspar-muscovite-quartz. The two species, $SnCl^+$ and $SnCl_2^0$, make up the total tin concentration in the fluid. Figure 12 shows that low f_{O_2} and high temperature are required for significant concentrations of tin in solution. For instance, at 500°C and QFM, the tin concentration is only 1 ppm. If the pH is decreased by 1 unit, that concentration is obtained at 400°C, QFM. That, however, is probably the lowest pH obtainable in this temperature range. Therefore, for the transport

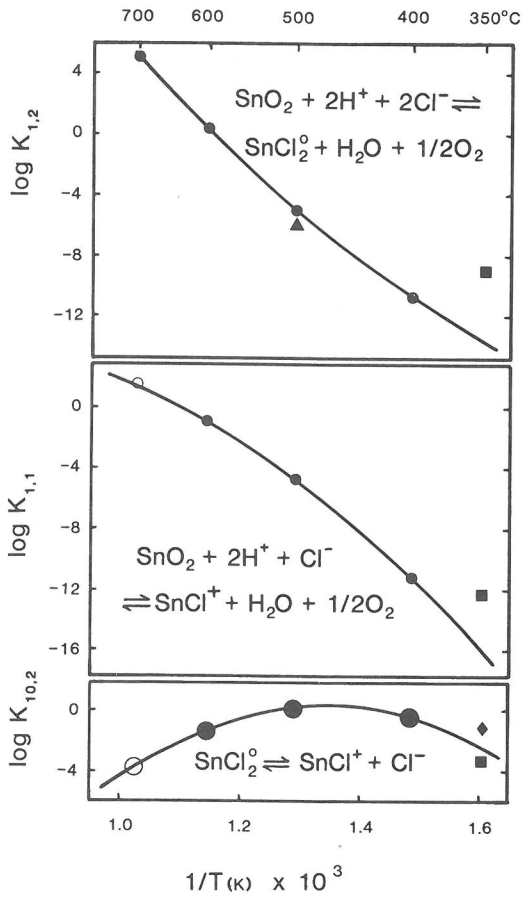

FIG. 10. Plot of log K vs. $1/T(K)$ for Reactions (1,1), (1,2), and (10,2). Round symbols are from this study (experimental) where $P = 1.5$ kb. The open round symbols represent a non-unique solution of the experimental data at 700°C as discussed in the text. The curves are fit to the solid round symbols only. The diamond is from the data of PATTERSON *et al.* (1981) and the squares are from JACKSON and HELGESON (1985a). Both are theoretical and for total pressure equal to the saturated vapor pressure of water. The triangle is from the experimental data of KOVALENKO *et al.* (1986) at 1.0 kb.

Table 5. Enthalpy and entropy of Reaction (10,2)

T (°C)	ΔH^0 (k J)	ΔS^0 (k J/K)
400	203.7	0.294
500	−83.56	−0.105
600	−305.0	−0.375
700	(−481.0)	(−0.566)

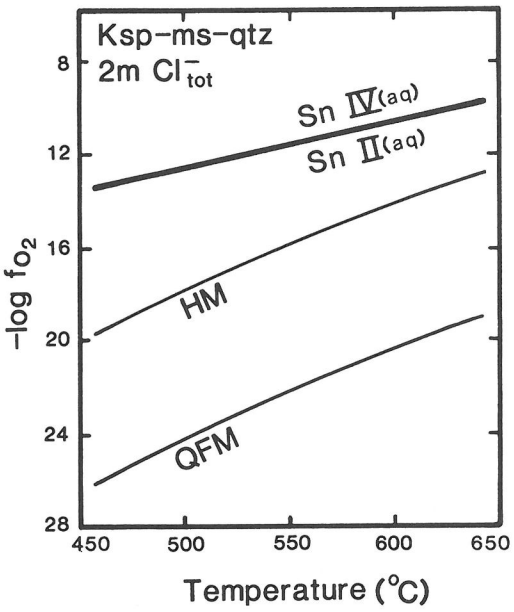

FIG. 11. Calculated relation between stannous (II) and stannic (IV) chloride complexes in natural hydrothermal fluids at 1.5 kb. Calculation is for a 2 m Cl_{total} solution with $\frac{K_{total}}{Na_{total}} = 0.15$ in equilibrium with the acid-buffer assemblage, K-feldspar-muscovite-quartz. Data are from this study, GUNTER and EUGSTER (1980), FRANTZ and MARSHALL (1984), QUIST and MARSHALL (1968), and FRANCK (1956).

of 1 ppm Sn or more in solution, it is necessary to have temperatures in excess of 400°C, pH at or below that of the K-feldspar-muscovite-quartz assemblage, and oxygen fugacity in the area of QFM-NNO. A decrease in temperature, increase in pH, or increase in oxygen fugacity can cause the deposition of cassiterite.

The solubilities of cassiterite and magnetite are compared in Fig. 13 where the data for magnetite are from CHOU and EUGSTER (1977). Although the solubilities of these two minerals are dependent on the same parameters, Fig. 13 shows that cassiterite solubility has a stronger dependence on oxygen fugacity and temperature than does magnetite solubility. At QFM, for instance, iron concentration decreases by about 4 orders of magnitude from 700 to 400°C whereas the tin concentration decreases by about 8 orders of magnitude at the same pH and chloride ion concentration. Consequently, at 500°C or lower, f_{O_2} near NNO, and free chloride ion concentration of 0.1 molar or more, Fe solutes greatly dominate Sn solutes in a fluid in equilibrium with magnetite + cassiterite.

Using the data presented here, the mechanisms responsible for cassiterite deposition can be quantitatively evaluated. Accepting $SnCl^+$ and $SnCl_2^0$ as the dominant species, precipitation is given by the reverse of Reaction (1),

$$SnCl_n^{2-n} + \tfrac{1}{2}O_2 + H_2O \rightarrow SnO_2 + 2H^+ + nCl^- \qquad (24)$$

Reaction (24) can be driven to the right by a drop in temperature, an increase in f_{O_2} and/or pH, and probably also a change in pressure, although the pressure dependency was not evaluated. For the conditions depicted in Fig. 12, for instance, a drop of 50°C can decrease the tin concentration in solution by as much as an order of magnitude. Similarly, a one unit increase in pH, all other parameters held constant, forces cassiterite to become supersaturated by two orders of magnitude. An increase in pH is most likely caused by interaction of the acidic ore fluids with the country rock, such as carbonates at Dachang (S.E. China) and Renison Bell (Tasmania) or schists at Panasqueira (Portugal). Acid neutralization by carbonates occurs through the reaction

$$CaCO_3 + H^+ \rightarrow Ca^{2+} + HCO_3^-, \qquad (25)$$

and can be monitored by the increased Ca^{2+} contents of fluid inclusions (KWAK and TAN, 1981a,b). In schists and granites, H^+ can be consumed

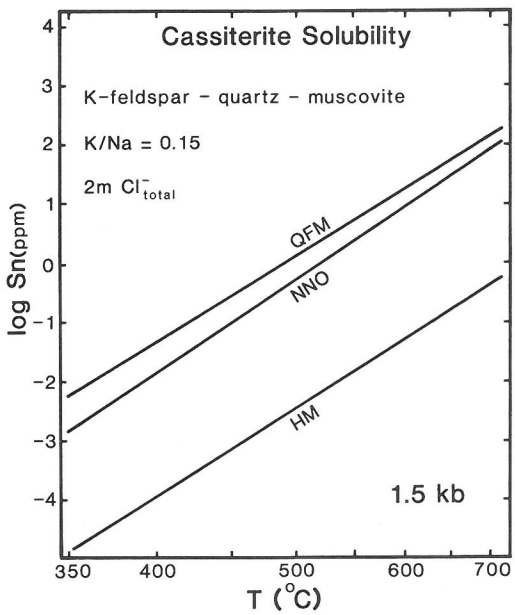

FIG. 12. Total solubility of cassiterite in natural hydrothermal fluids at 1.5 kb as a function temperature and f_{O_2}. Fluid is the same as in Fig. 11.

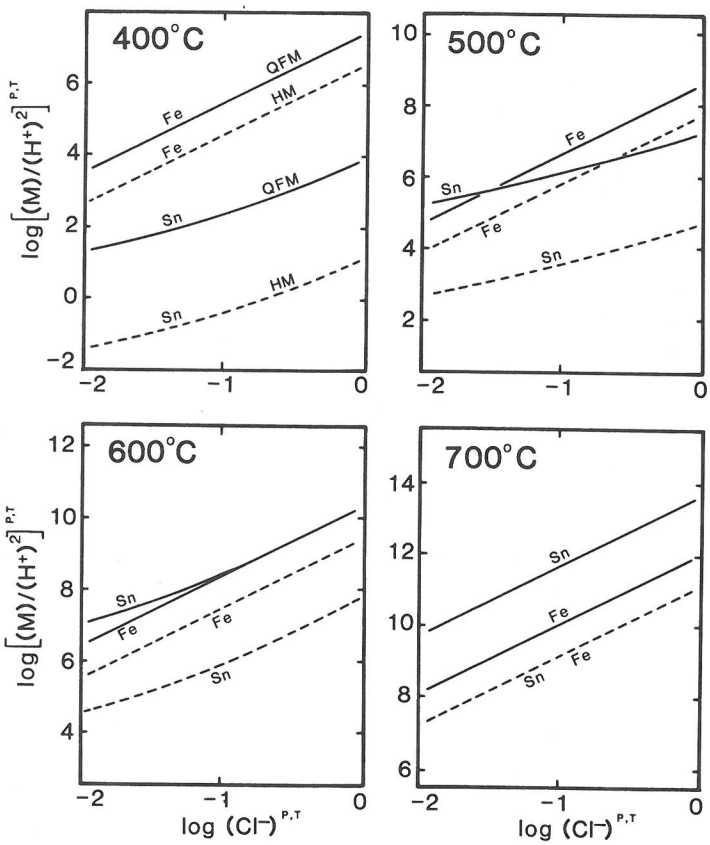

FIG. 13. Solubility diagram for magnetite and cassiterite at 400 to 700°C. Magnetite solubility is at 2 kb from the data of CHOU and EUGSTER (1977). Cassiterite solubility is at 1.5 kb from this study. Solid curves are calculated at QFM and dashed curves are at HM. (M) represents the total concentration of either Sn or Fe. The concentrations of H^+ and Cl^- are for the free ions at P and T.

through the alteration of feldspars to muscovite by the reaction (HEMLEY, 1959),

$$3KAlSi_3O_8 + 2H^+ \rightarrow KAl_3Si_3O_{10}(OH)_2 + 6SiO_2 + 2K^+. \quad (26)$$

Indeed, cassiterite-quartz veins frequently are lined with coarse muscovite selvages.

A decrease in chloride molality also can initiate cassiterite deposition and it is most easily accomplished by mixing of ore fluids with dilute, meteoric waters. Such mixing has been inferred for many hydrothermal systems from stable isotope studies (see for instance PATTERSON *et al.*, 1981; and JACKSON *et al.*, 1982).

Since the oxidation state of tin is 2 in solution and 4 in cassiterite, oxidation is an essential requirement for cassiterite deposition. In principle, an increase in f_{O_2} can be accomplished by a differential loss of hydrogen, but as pointed out elsewhere (EUGSTER, 1986), coupled redox reactions without a net transfer of oxygen are probably more effective. Simultaneous precipitation of cassiterite and arsenopyrite, and of cassiterite and sulfides are examples (HEINRICH and EADINGTON, 1986; EUGSTER, 1986):

$$3SnCl_2^0 + 2H_3AsO_3^0 + 2FeCl_2^0 + 2H_2S^0 \rightarrow 3SnO_2 + 2FeAsS + 10HCl^0, \quad (27)$$

and

$$7SnCl_2^0 + FeCl_2^0 + 2H_2SO_4^0 + 6H_2O \rightarrow 7SnO_2 + FeS_2 + 16HCl^0. \quad (28)$$

The acidity produced by Reactions (27) and (28) can be consumed by reactions such as (25) and (26).

CONCLUSIONS

Solubility experiments in supercritical HCl solutions can provide the information necessary to identify the dominant aqueous species and to for-

mulate and quantify mineral dissolution-precipitation reactions. This leads to a better understanding of the processes responsible for mineral transport and deposition. From cassiterite solubility experiments we found that the dominant tin-chloride species in supercritical HCl solutions are $SnCl^+$, and $SnCl_2^0$ under geologically reasonable pH and f_{O_2} conditions from 400 to 700°C, 1.5 kb. The species, $SnCl_3^+$, has also been identified at a lower pH and higher f_{O_2} from 500 to 600°C. For the transport of significant quantities of tin in hydrothermal solutions, high temperature, low f_{O_2}, and low pH are required. These conditions are reflected in many natural tin deposits. Deposition of cassiterite can be initiated by a drop in temperature, a rise in pH through reaction with wallrock, a redox reaction with coupled precipitation, or mixing with dilute meteoric waters. Although these mechanisms have been suggested previously, solubility data presented in this paper permit quantitative evaluation of individual processes.

Acknowledgements—G. A. Wilson wishes to express his gratitude for the inspiration and guidance of Professor Hans P. Eugster. Hans will always be remembered.

Many conceptual and technical difficulties were overcome through discussions with Eugene Ilton, Sigudur Gislason, Sheng-Yuan Wang, I-Ming Chou, Terry Seward, Phil Candela, and Scott Wood. Dimitri Sverjensky is also gratefully acknowledged for sharing with us his insight. This manuscript was greatly improved thanks to constructive reviews by Phil Candela, I-Ming Chou, and Jeremy Fein. This work represents part of the senior author's Ph.D. dissertation at The Johns Hopkins University. Support was provided by National Science Foundation grants EAR 82-06177 and EAR 84-11050.

REFERENCES

BAUMANN L., STEMPROK M., TISCHENDORF G. and ZOUBEK V. (1974) Metallogeny of tin and tungsten in the Krusne Hory-Erzgebirge. Geol. Survey, Prague. 66p.

BEVINGTON P. R. (1969) *Data Reduction and Error Analysis for the Physical Sciences.* 336 pp. McGraw-Hill, New York.

BRAY C. J. and SPOONER E. T. C. (1983) Sheeted vein Sn-W mineralization and greisenization associated with economic kaolinitization, Goonbarrow china clay pit, St. Austell, Cornwall, England: geologic relationships and geochronology. *Econ. Geol.* **78,** 1064–1089.

CHOU I-M. and EUGSTER H. P. (1977) Solubility of magnetite in supercritical chloride solutions. *Amer. J. Sci.* **277,** 1296–1314.

CHRISTIANSEN E. H., SHERIDAN M. J. and BURT D. M. (1986) The geology and geochemistry of Cenozoic topaz rhyolites from the western United States. *Geol. Soc. Amer. Spec. Paper* **205.**

CLARK A. H., PALMA V. V., ARCHIBALD D. A., FARRAR E., ARENAS M. J. F. and ROBERTSON R. C. R. (1983) Occurrence and age of tin mineralization in the Cordillera Oriental, Southern Peru. *Econ. Geol.* **78,** 514–520.

COLLINS P. L. F. (1981) The geology and genesis of the Cleveland tin deposit, western Tasmania: fluid inclusion and stable isotope studies. *Econ. Geol.* **76,** 365–392.

CRERAR D. A., SUSAK N. J., BORSIK M. and SCHWARTZ S. (1978) Solubility of the buffer assemblage pyrite + pyrrhotite + magnetite in NaCl solutions from 200 to 300°C. *Geochim. Cosmochim. Acta* **42,** 1427–1437.

DADZE T. P., SOROKHIN V. I. and NEKRASOV I. Y. (1982) Solubility of SnO_2 in water and in aqueous solutions of HCl, HCl + KCl, and HNO_3 at 200 to 400°C and 101.3 Mpa. *Geochem. Internat.* **18,** 142–152.

DRAPER N. R. and SMITH H. (1981) *Applied Regression Analysis.* (second edition). 709 pp. John Wiley & Sons.

EADINGTON P. J. (1982) Calculated solubilities of cassiterite in high temperature hydrothermal brines, and some applications to mineralization in granitic rocks and skarns. *Proc. First Int. Symp. on Hydrothermal Reactions* (ed. S. SOMIYA), pp. 335–345. Tokyo Inst. Tech.

EADINGTON P. J. (1983) A fluid inclusion investigation of ore formation in a tin-mineralized granite, New England, New South Wales. *Econ. Geol.* **78,** 1204–1221.

EUGSTER H. P. (1986) Minerals in hot water. *Amer. Mineral.* **71,** 655–673.

EUGSTER H. P., CHOU I-M. and WILSON G. A. (1987) Mineral solubility and speciation in supercritical chloride fluids. In *Hydrothermal Experimental Techniques* (eds. G. C. ULMER and H. L. BARNES), pp. 1–19. John Wiley & Sons.

EUGSTER H. P. and WONES D. R. (1962) Stability relations of the ferruginous biotite, annite. *J. Petrol.* **3,** 82–125.

EVANS A. M. (EDITOR) (1982) *Metallization Associated with Acid Magmatism.* 385 pp. John Wiley & Sons.

FRANCK E. U. (1956) Hochverdichteter Wasserdampf III. Ionendissoziation von KCl, KOH, und H_2O in überkritischem Wasser. *Z. Phys. Chem.* **8,** 192–206.

FRANTZ J. D. and MARSHALL W. L. (1984) Electrical conductances and ionization constants of salts, acids, and bases in supercritical aqueous fluids: I. Hydrochloric acid from 100 to 700°C and at pressures to 4000 bars. *Amer. J. Sci.* **284,** 651–667.

GUNTER W. D. and EUGSTER H. P. (1980) Mica-feldspar equilibria in supercritical alkali chloride solutions. *Contrib. Miner. Petrol.* **75,** 235–250.

HAAPALA I. and KINNUNEN K. (1982) Fluid inclusion evidence on the genesis of tin deposits. In *Metallization Associated with Acid Magmatism* (Ed. A. M. EVANS), pp. 101–110. John Wiley & Sons.

HALLS C. (EDITOR) (1985) *High Heat Production Granites, Hydrothermal Circulation and Ore Genesis.* Institute of Mining and Metallurgy. London. 593 pp.

HARTLY F. R., BURGESS C. and ALCOCK R. M. (1980) *Solution Equilibria.* 361 pp. Ellis Horwood Limited, Halstead Press.

HEINRICH C. A. and EADINGTON P. J. (1986) Thermodynamic predictions of the hydrothermal chemistry of arsenic, and their significance for the paragenetic sequence of some cassiterite-arsenopyrite-base metal sulfide deposits. *Econ. Geol.* **81,** 511–529.

HEMLEY J. J. (1959) Some mineralogical equilibria in the system K_2O-Al_2O_3-SiO_2-H_2O. *Amer. J. Sci.* **257,** 241–270.

ISHIHARA S. and TAKENOUCHI S. (EDITORS) (1980) *Granite Magmatism and Related Mineralization.* Japan Soc. Mining Geol. Spec. Issue **8,** Tokyo, 247p.

JACKSON K. J. and HELGESON H. C. (1985a) Chemical and thermodynamic constraints on the hydrothermal transport and deposition of tin: I. Calculations of the solubility of cassiterite at high pressures and temperatures. *Geochim. Cosmochim. Acta* **49,** 1–22.

JACKSON K. J. and HELGESON H. C. (1985b) Chemical and thermodynamic constraints on the hydrothermal transport and deposition of tin: II. Interpretation of phase relations in the southeast Asian tin belt. *Econ. Geol.* **80,** 1365–1378.

JACKSON N. L., HALLIDAY A. N., SHEPPARD S. M. F. and MITCHELL J. G. (1982) Hydrothermal activity in the St. Just mining district, Cornwall, England. In *Metallization Associated with Acid Magmatism* (ed. A. M. EVANS), pp. 137–179. John Wiley & Sons.

JOHANSSON L. (1970) Iteration procedures in solution chemistry with special reference to solubility measurements. *Acta Chemica. Scandinavica* **24,** 1572–1578.

KELLY W. C. and RYE R. O. (1979) Geologic, fluid inclusion, and stable isotope studies of the tin-tungsten deposits of Panasqueira, Portugal. *Econ. Geol.* **74,** 1721–1819.

KELLY W. C. and TURNEAURE F. S. (1970) Mineralogy, paragenesis and geothermometry of the tin and tungsten deposits of the Eastern Andes, Bolivia. *Econ. Geol.* **65,** 609–680.

KLINSTOVA A. P. and BARSUKOV V. L. (1973) Solubility of cassiterite in water and in aqueous NaOH solutions at elevated temperatures. *Geochem. Int.* **10,** 540–547.

KLINTSOVA A. P., BARSUKOV V. L., SHEMARYKINA T. P. and KHODAKOVSKIY I. L. (1975) Measurement of the stability constants for Sn(IV) hydrofluoride complexes. *Geochem. Int.* **12,** no. 2, 207–215.

KOVALENKO, N. I., RYZHENKO B. N., BARSUKOV V. L., KLINTSOVA A. P., VELYUKHANOVA T. K., VOLYNETS M. P. and KITAYEVA L. P. (1986) The solubility of cassiterite in HCl and HCl + NaCl (KCl) solutions at 500°C and 1000 atm under fixed redox conditions. *Geochem. Int.* **23,** No. 7, 1–16.

KWAK T. A. P. (1983) The geology and geochemistry of the zoned, Sn-W-F-Be skarns at Mt. Lindsay, Tasmania, Australia. *Econ. Geol.* **78,** 1440–1465.

KWAK T. A. P. (1987) *W-Sn Skarn Deposits and Related Metamorphic Skarns and Granitoids.* 452 pp. Elsevier.

KWAK T. A. P. and TAN T. H. (1981a) The geochemistry of zoning in skarn minerals at the King Island (Dolphin) mine. *Econ. Geol.* **76,** 468–497.

KWAK T. A. P. and TAN T. H. (1981b) The importance of $CaCl_2$ in fluid composition trends—evidence from the King Island (Dolphin) skarn deposit. *Econ. Geol.* **76,** 955–960.

NEKRASOV I. Y. and LADZE T. P. (1973) Solubility of cassiterite in silicic chloride solutions at 300°C and 400°C. *Doklady Akad. Nauk SSSR* **213,** 145–147.

NORMAN D. I. and TRANGCOTCHASAN Y. (1982) Mineralization and fluid inclusion study of the Yod Nam tin mine, southern Thailand. In *Metallization Associated with Acid Magmatism* (Ed. A. M. EVANS), pp. 261–272. John Wiley & Sons.

PABALAN R. T. (1986) Solubility of cassiterite (SnO_2) in NaCl solutions from 200°C–350°C, with geologic applications. Ph.D. Dissertation. The Pennsylvania State University, University Park, Pennsylvania.

PATTERSON D. J., OHMOTO H. and SOLOMON M. (1981) Geologic setting and genesis of cassiterite-sulfide mineralization at Renison Bell, western Tasmania. *Econ. Geol.* **76,** 393–438.

PETERSON E. U. (1986) Tin in volcanogenic massive sulfide deposits: An example from the Geco mine, Manitouwadge District, Ontario, Canada. *Econ. Geol.* **81,** 323–342.

PUCHNER C. C. (1986) Geology, alteration and mineralization of the Kougarok Sn deposit, Seward Peninsula, Alaska. *Econ. Geol.* **81,** 1775–1794.

QUIST A. S. and MARSHALL W. L. (1968) Electrical conductances of aqueous sodium chloride solutions from 0 to 800°C and at pressures to 4000 bars. *J. Phys. Chem.* **72,** 684–703.

RAYSON G. D. and HOLCOMBE J. A. (1982) Tin atom formation in a graphite furnace atomizer. *Anal. Chim. Acta* **136,** 249–260.

REES C. E. (1984) Error propagation calculations. *Geochim. Cosmochim. Acta* **48,** 2309–2311.

ROEDDER E. (1984) *Fluid Inclusions. Mineral. Soc. Amer., Rev. in Mineral.* **12,** 644p.

ROSSOTTI F. J. C. and ROSSOTTI H. (1961) *The Determination of Stability Constants.* 425 pp. McGraw-Hill.

SEWARD T. M. (1973) Thio complexes of gold and the transport of gold in hydrothermal ore solutions. *Geochim. Cosmochim. Acta* **37,** 379–399.

SEWARD T. M. (1976) The stability of chloride complexes of silver in hydrothermal solutions up to 350°C. *Geochim. Cosmochim. Acta* **40,** 1329–1341.

SEWARD T. M. (1981) Metal complex formation in aqueous solutions at elevated temperatures and pressures. In *Chemistry and Geochemistry of Solutions at High Temperatures and Pressures* (eds. D. T. RICKARD and F. E. WICKMAN), *Phys. and Chem. of the Earth* **13 & 14,** 113–132.

SILLITOE R. H., HALLS C. and GRANT J. N. (1975) Porphyry tin deposits in Bolivia. *Econ. Geol.* **70,** 913–927.

SLAVIN W., MANNING D. C. and CARNICK G. R. (1981) The stabilized temperature platform furnace. *Atomic Spectrosc.* **2,** 137–145.

SUN S-S. and EADINGTON P. J. (1987) Oxygen isotope evidence for the mixing of magmatic and meteoric waters during tin mineralization in the Mole Granite, New South Wales, Australia. *Econ. Geol.* **82,** 43–52.

TAYLOR R. G. (1979) *Geology of Tin Deposits.* 543 pp. Elsevier.

VON GRUENEWALDT G. and STRYDOM J. H. (1985) Geochemical distribution patterns surrounding tin-bearing pipes and the origin of the mineralizing fluids at the Zaaiplaats tin mine, Potgietersrus District. *Econ. Geol.* **80,** 1201–1211.

WILSON G. A. (1986) Cassiterite solubility and metal-chloride speciation in supercritical solutions. Ph.D. Dissertation. The Johns Hopkins University, Baltimore, Maryland.

WILSON G. A. and EUGSTER H. P. (1984) Cassiterite solubility and metal-chloride speciation in supercritical solutions (abstr.). *Geol. Soc. Amer. Ann. Meeting Abstr. Prog.* **16,** 696.

WOOD S. A. and CRERAR D. A. (1985) A numerical method for obtaining multiple linear regression parameters with physically realistic signs and magnitudes: Applications to the determination of equilibrium constants from solubility data. *Geochim. Cosmochim. Acta* **49,** 165–172.

ZHANG Z. and LI X. (1981) Studies on mineralization and composition of Dachang ore field, Guangxi Province, China. *Geochimica* **1,** 74–86.

ZAW U. K. and DAW K. M. T. (1983) A note on a fluid inclusion study of tin-tungsten mineralization at Mawchi Mine, Kayah State, Burma. *Econ. Geol.* **78,** 530–534.